Chaos, Solitons and Fractals 173 (2023) 113697

Contents lists available at ScienceDirect

Chaos, Solitons and Fractals

journal homepage: www.elsevier.com/locate/chaos

Quantifying the potentiality for polarization in opinion networks

Alejandro Carballosa [a,b], Álvaro Crego [a], Alberto P. Muñuzuri [a,b,*]

[a] Group of Nonlinear Physics, Fac. Physics, University of Santiago de Compostela, 15782 Santiago de Compostela, Spain
[b] Galician Center for Mathematical Research and Technology (CITMAga), 15782 Santiago de Compostela, Spain

ARTICLE INFO

Keywords:
Opinion formation
Complex networks
Opinion polarization
Turing

ABSTRACT

Polarization in debates and social networks is a phenomenon clearly present in modern societies that strongly modifies the way we relate as communities. Regardless of the importance of this phenomenon, there is not a clear explanation yet for its emergence or a suitable parameter to quantify it. Here, we present a methodology based on the Turing instability, a frequent mechanism in Nature which explains differentiation processes, that maps the conditions needed for a given network to undergo polarization of opinions. From this mapping, we measure the likelihood of the system's nodes to differentiate each other or, in other terms, the degree of polarization of the network.

1. Introduction

Someone said that the face is the mirror of the soul, in this manuscript we try to address the question: is the social network the mirror of our society? Or, in other words, can the network structure give information about the type of society we live in? and can we quantify those differences with a limited set of measurable parameters?

Nowadays, most of our communications, somehow, end up in a social network, if you do not contribute to the network, it is almost as if you do not exist. Thus, it just seems straight forward that understanding how the network works may help to control the opinion of such society. Proof of this is the large number of studies [1] devoted to this topic and even the growing interest of contemporary politicians to understand and control the network as a key to win elections.

Within this context, it is of high interest the concept of opinion polarization [1], the intrinsic property of a topic to reach a state where the opinions about it are equally distributed in opposing positions. In particular, the study of political polarization has been the focus of research for plenty of decades [2–6] and in the debate on whether polarization levels have been increasing or not, scientific literature suggests that they do [7–10]. On many occasions any issue (sometimes even trivial ones) triggers a polarized response and the opinion splits equally into two opposing factions.

The role of the social networks in this increasing degree of polarization is highly difficult to measure and many books and articles point towards their influence [11–13], although a recent study shows that there is not a clear association between faster growth in political polarization and greater internet use [14]. It is clear though, that the boom of social media has broken the boundaries of physical distances and increased the social interaction rates. Daily discussions on multiple topics compete for the attention and engagement of individuals [15,16], creating datasets of rich and complex networks that can be thoroughly analyzed in the search and measure of polarized structures [17–19].

Attempts to understand these opinion formation processes through mathematical modelling have been many and they are usually focused on how the network structure affects the opinion dynamics. A seminal work by DeGroot [20] showed with a simple model how the averaged interaction of agents with different initial opinions tends to decrease the overall disagreement reaching a consensus. This is not a very realistic scenario, however, but introducing the innate belief of the agents (a persistent state of mind) with a set of weights in the averaging process that accounts for the network influence suffices to allow for disagreement states [21]. Going further, it has been shown that homophily [22], the tendency of individuals to connect with other individuals of similar thinking, results in a natural mechanism that can lead to polarized structures [23,24], but it is not always a sufficient condition for it [25]. Another empirical observation found in several polarized social networks is the existence of echo chambers [26–29], a reinforcement of one's opinions in time by other individuals or any kind of media. Modelling echo chambers in combination with homophily [30] does seem to lead to a more robust model, where metastable polarized states can be reached from a situation of global consensus. Alternatively, other routes to polarization include the idea of bias assimilation [25,31], link recommender systems [32,33] and the importance of the topic's

* Corresponding author at: Group of Nonlinear Physics, Fac. Physics, University of Santiago de Compostela, 15782 Santiago de Compostela, Spain.
E-mail address: alberto.perez.munuzuri@usc.es (A.P. Muñuzuri).

https://doi.org/10.1016/j.chaos.2023.113697
Received 11 March 2023; Received in revised form 7 June 2023; Accepted 8 June 2023
Available online 21 June 2023
0960-0779/© 2023 The Authors. Published by Elsevier Ltd. This is an open access article under the CC BY license (http://creativecommons.org/licenses/by/4.0/).

controversy [34,35].

On the other hand, the Turing instability [36] has been known to provide a mechanism for spontaneous diffusion-induced symmetry breaking that has been widely used to explain pattern formation mechanisms in Biology [37] and, lately, to explain some phenomena in the context of bilingualism dynamics [38]. In this paper we aim to relate the ability of a system to exhibit Turing instability with the study of opinion polarization. Since rumor spreading and opinion formation are in nature diffusive phenomena, it is reasonable that the Turing instability could help to better understand these processes.

With a suitable dynamical model and network diffusion in it, we map the parameter space in which the opinion formation process undergoes the instability from a neutral stable state (consensus) to another differentiated stationary state, where nodes acquire a different opinion and, if the dynamical parameters are adequate, leave the system in a polarized state. We must remark here that our model differs from others that study polarization dynamics in the sense that the opposing opinions do not exist in the absence of diffusion and it is only possible because of it. Our model considers then a more relaxed definition of polarization in which nodes don't end up occupying opposing opinions known beforehand, for example 1 and -1, and rather examines the onset of the polarization itself. In other words, we believe that the Turing instability could help to explain why in the presence of the network the consensus is broken and locate the conditions needed for it. To quantify this feature, we measure the size of the parameter space for different network topologies and propose it as a quantitative indicator of the onset of polarization for each one. Besides, since this parameter space is obtained through analytical computations based on linear stability analysis, our descriptor does not require to perform extensive simulations and is computationally affordable and efficient. However, this implies some limitations too. On one side, since it does not know the final state of the system, it cannot distinguish if one of the opposing opinions is much more populated than the other and therefore does not give a measure of how much polarized the state is. Thus, it reduces mainly to describe whether the differentiation of opinions will occur or not (the onset to break consensus) because of the network structure. Also, since the computations of the descriptor rely on a fixed adjacency matrix that describes the said structure, the networks considered here are static. Or, in other words, the observation times considered are short compared with the times needed for a network to significantly evolve. We are aware that the opinion formation process is best described through an adaptive network scheme [39] that could be able to incorporate all the previously mentioned approaches that lead to polarization. However, rather than studying the opinion formation process in itself, our aim focuses on characterizing the potentiality of polarization of a given network in a specific moment in time. If one were to know the evolution of the adjacency matrix in time, the descriptor could be computed for each known time step to study if this polarization potential shows certain temporal patterns.

Our results show that the connectivity distribution and specially its dispersion are key in the differentiation process, as a previous work had already observed for the general case of Turing patterns in other biological models [40]. In this context, our descriptor shows that a network model with scale-free distribution presents a more continuous and extensive transition to the differentiated state, in which nodes become polarized in an orderly fashion attending to their connectivity. Nodes with larger connectivities become polarized in a broader region of parameter space, and although do not leave the whole network in a polarized state they induce some noise in it. This could be interpreted as these highly connected nodes participating more in the conversation because they have something different to say, trying to spread their views to the whole network. On the other hand, for networks with finite, small dispersion in their connectivity distribution, the Turing instability region is less accessible in the parameter space but their Turing patterns reflect clearer polarized structures where almost all nodes differentiate into two extreme opinion clusters. To contrast the results of our descriptor, we also carried out extensive numerical simulations and measured the degree of polarization with the index proposed by [19]. We found that our descriptor clearly outlines the region in the parameter space in which consensus is broken and nodes start to differentiate, and measured then how different topological features of the networks affected our results.

In the following, we describe our model and our stability descriptor in Section 2, the results we obtain for different network topologies in Section 3 and some final conclusions in Section 4.

2. Model

Let us define a system of N interacting individuals where we introduce the competition of two opposing ideas or opinions, u and v, that are able to diffuse across the links of a complex network. The innate belief of the individuals evolve in time according to the functions $f(u_i, v_i) = u_i(a_1 - b_1 u_i - c v_i)$, and $g(u_i, v_i) = v_i(a_2 - b_2 v_i + c\, u_i)$, with the dynamical parameters controlling how they grow (a), decrease (b) and compete (c) inside each individual. These set of dynamics were previously used for studying how different network topologies affect the coexistence of two languages [38], where one of them is favored by the sign of the competition term. Let us define now the adjacency matrix of the network A_{ij}, and the Laplacian matrix $L_{ij} = A_{ij} - \delta_{ij} k_i$, with $k_i = \sum_j^N A_{ij}$, the connectivity of node i. Thus, the individuals will update their opinions based on their neighbors as $\epsilon \sum_j^N A_{ij} d(u_j - u_i) = \epsilon \sum_j^N L_{ij} d\, u_j$, with d being the diffusion coefficient according to Fick's law and ϵ the influence that the network exerts on the innate beliefs. In this sense, the latter can be understood both in terms of a network influence or in how appealing or engaging is a certain topic to the individuals. Finally, it is also described in several works [38,41–44] that for some reactive-diffusion models the addition of cross-diffusion into the system is essential for the emergence and control of spatial and spatiotemporal structures. It represents a mechanism by which the concentration gradient of one variable induces an opposite gradient from the other, a feature that makes it very suitable for modelling competing species. In our case, it translates to the opinion variables diffusing to where the concentration of the opposing opinion is lower, favoring the communication flows and clusters of like-minded individuals. In this sense, could the system accounts for the concept of homophily from the point of view of opinion dynamics, rather than from the network structure. The cross-diffusion is then both a necessary condition and a control parameter of the Turing instability, given by the parameters d_{uv} and d_{vu}. To sum up, the time evolution of the opinions is governed by the following equations,

$$\begin{cases} \dfrac{du_i}{dt} = f(u_i, v_i) + \epsilon \displaystyle\sum_{j=1}^{N} L_{ij} \left[u_j \left(d + d_{uv} v_j \right) \right] \\ \dfrac{dv_i}{dt} = g(u_i, v_i) + \epsilon \displaystyle\sum_{j=1}^{N} L_{ij} \left[v_j \left(d + d_{vu} u_j \right) \right] \end{cases} \tag{1}$$

In absence of diffusion, each individual i will evolve its opinion until it reaches one of the fixed points of the system (u^0, v^0), which can be computed analytically as those points where $\dot{u}_i = \dot{v}_i = 0$. When diffusion is turned on, the system will either return to one of the previous fixed points, simulating the reach of a consensus, or achieve a new stationary state where individuals in the network adopt new extreme positions by means of the Turing instability. In the end, we have an internal process whose natural tendency is to return to equilibrium while a tunable network influence tries to disrupt this state. Note that our model does not distinguish between intrinsic preferences so the emergence of polarization is purely a collective phenomenon where social connectivity (and therefore diffusion) is crucial.

In this way, the Turing instability exemplifies the ability to break the system's homogeneity and, consequently, introduce polarization or, at

least, differentiation in a natural way. Both the dynamical parameters and network topology strongly affect the model capability to undergo the instability and, thus, the region in the control parameter space where it is found. In order to inspect the instability, we carry out a linear stability analysis of the stable stationary state with respect to non-uniform perturbations. Expanding over the set of Laplacian eigenvectors $\Phi^{(\alpha)} = \left(\phi_1^{(\alpha)}, \ldots, \phi_N^{(\alpha)}\right)$, with $\alpha = 1, \ldots, N$ the Laplacian modes, we can write these perturbations as $\delta u_i(t) = \sum_\alpha^N exp(\lambda_\alpha t)\phi_i^{(\alpha)}$ [45]. The stability of the system is then determined by the exponents λ_α: if their sign is negative, the perturbation will decay and the state will remain stable. On the contrary, if one of the λ_α are positive, it is a sign that the state has become unstable and the perturbation grows exponentially in time. Thus, these exponents are usually denoted as the linear *growth rates* of the system [40,45], and we present their analytical derivation in the *Supplementary Information* section *S1*. They depend mostly on the Laplacian eigenvalues Λ_α and the network influence ϵ, and since both of these parameters control the degree of diffusion the resulting positive growth rates can be used as a trace of the instability region. We will use the size of this region as a quantitative value of the degree of polarization, meaning that the larger the region, the more prone to polarization the network will be. Note that this method allows us to characterize if a given network is capable of sustaining different opinions (expressed with different stationary states) and a non-homogeneous distribution of them along the network.

We will also consider the polarization index proposed by [19] to contrast our results and analyze the polarized structures given by our model. Given the previous definition that a polarized state is that in which the opinions are equally distributed in opposing positions, we need to measure both the population of individuals in each position and the ideological distance between them. As we mentioned, if the network undergoes the Turing instability, the new ideological positions will appear above and below the fixed point of the system u^0 Thus, we define N^- as the relative population of individuals with opinions below the fixed point ($u_i < u^0$) and N^+ the relative population of individuals above it ($u_i > u^0$). The normalized difference in population sizes will then be given by

$$\Delta N = \frac{|N^+ - N^-|}{N} \tag{2}$$

Similarly, to measure the distance between the opinion clusters we start by considering the difference between the average value of each opinion cluster, divided by the difference of the maximum values in the opinion distribution:

$$\eta = \frac{\langle u^+ \rangle - \langle u^- \rangle}{u_{Max} - u_{Min}} \tag{3}$$

Finally, we can use these two equations to measure polarization as a function of the population differences and the distance between them, writing the polarization index as [19].

$$\mu = (1 - \Delta N) \cdot \eta \tag{4}$$

with $0 \leq \mu \leq 1$. When the resulting opinion distribution is clearly bimodal, equally populated and with each opinion center located at each extremal value, the polarization index will be equal to 1. On the other hand, μ will be zero or near zero when opinions do not differentiate or, even if they had acquired new extremal values, one of the clusters is more heavily populated than the other.

3. Results

First, we describe the behavior of the model as a function of the control parameters that best trigger the instability: the competition rate c, the cross diffusion coefficient d_{vu} and the network influence ϵ. First, we show a glimpse of the simulations and the parameter-dependence of the Turing instability through Fig. 1. We integrate Eq. (1) for a system of $N = 1000$ nodes initialized around the fixed point of the system (u^0, v^0) with a small random perturbation. For low values of the network influence (see upper part of panel (a)), the model with nodes connected following an Erdos-Renyi (ER) network [46] does not undergo the instability and every node returns to the fixed point, reaching what we could identify as a consensus state. On the other hand, in a Barabasi-Albert (BA) network [47], we observe that a few nodes with the highest connectivities have adopted new differentiated positions that induce a small noise in the rest of the network (which remains around the consensus value), outlining the onset of polarization. If we increase now the network influence sufficiently, to $\epsilon = 0.5$, both networks exhibit two differentiated states non-homogeneously distributed along the network nodes and achieve near perfect polarization on almost every node (see lower part of panel (a)), jumping to either the state at $u_i \sim u_{max} = 25$ or $u_i \sim u_{min} = 0$. Attending now to the respective growth rate distributions in panel (b), we can understand in each case why the networks underwent or not the instability. The opinion differentiation starts at a certain critical eigenvalue Λ_{α_c}, from which the growth rates become positive, and panel (b) clearly shows that in the case of the ER with low network influence this eigenvalue is not reached. As we shall explicit later on, if we increase the average connectivity of the ER, this would lead also to an increase in the eigenvalues and therefore it would also be possible for this topology to surpass the critical threshold. In the case of the BA network, the scale-free property [48] and the spread distribution of connectivities allows the existence of larger Laplacian eigenvalues that overcome the critical threshold even for small values of the network influence. For the sake of comparison and conceptual highlighting, our networks have been built with a fixed average connectivity of $\langle k \rangle \simeq 10$ and, unless stated otherwise, the reaction and diffusion parameters of Eq. (1) are fixed to $a_1 = a_2 = 2.0$, $b_1 = 0.08$, $b_2 = 0.3$ and $d = 0.001$.

With the growth rates (GR) as a tracer of the Turing instability, we measure region in the parameter space where their value is positive and characterize the networks' capability to induce opinion polarization. We will consider now systems of $N = 5000$ nodes and besides the BA and ER models, we will also consider the Watts-Strogatz (WS) topology [49] because of its even lower connectivity dispersion and its capability to tune the average path length of the graph from the probability of random shortcuts in the network. Since the average path length ℓ is the average distance between all pairs of nodes, the larger it is the longer will take the diffusion process. Considering the total number of performed simulations (covering the whole parameter space), we define the *Turing area* of the network as the fraction of these simulations where the Turing instability appeared. Panels (a to c) of Fig. 2 clearly shows that the capability to destabilize the system can be easily mapped with this measure and used to distinguish between different network structures. The larger dispersion in the connectivity of the scale-free topology given by the BA model plays a crucial role in the appearance of the Turing instability [40], finding that for small values of the network influence ($\epsilon = 0.1$) it is considerably larger than for the ER and WS. For these cases, whose connectivity follow a Gaussian distribution with small dispersion, their spectrum of eigenvalues is more compact and their eigenvectors are more delocalized, having their normalization weights distributed uniformly. Thus, the critical mode here is only reached when the dynamical parameters of the model are high enough, or the network influence is significantly increased (panels g-i). This is directly related to the eigenvalues and eigenvectors of the Laplacian matrixand their dependence on the network connectivity. The connectivity distribution of the scale-free topology allows for a wider spectrum of eigenvalues, which makes it easier to reach the critical mode α_c and the positive solutions of the GR. On the other hand, the eigenvectors associated to nodes with higher degrees have their normalization weights concentrated on a small subset of their components (they are "localized"), and this property is what makes these nodes to differentiate faster [40].

Attending now to the polarization index μ computed as in Eq. (4),

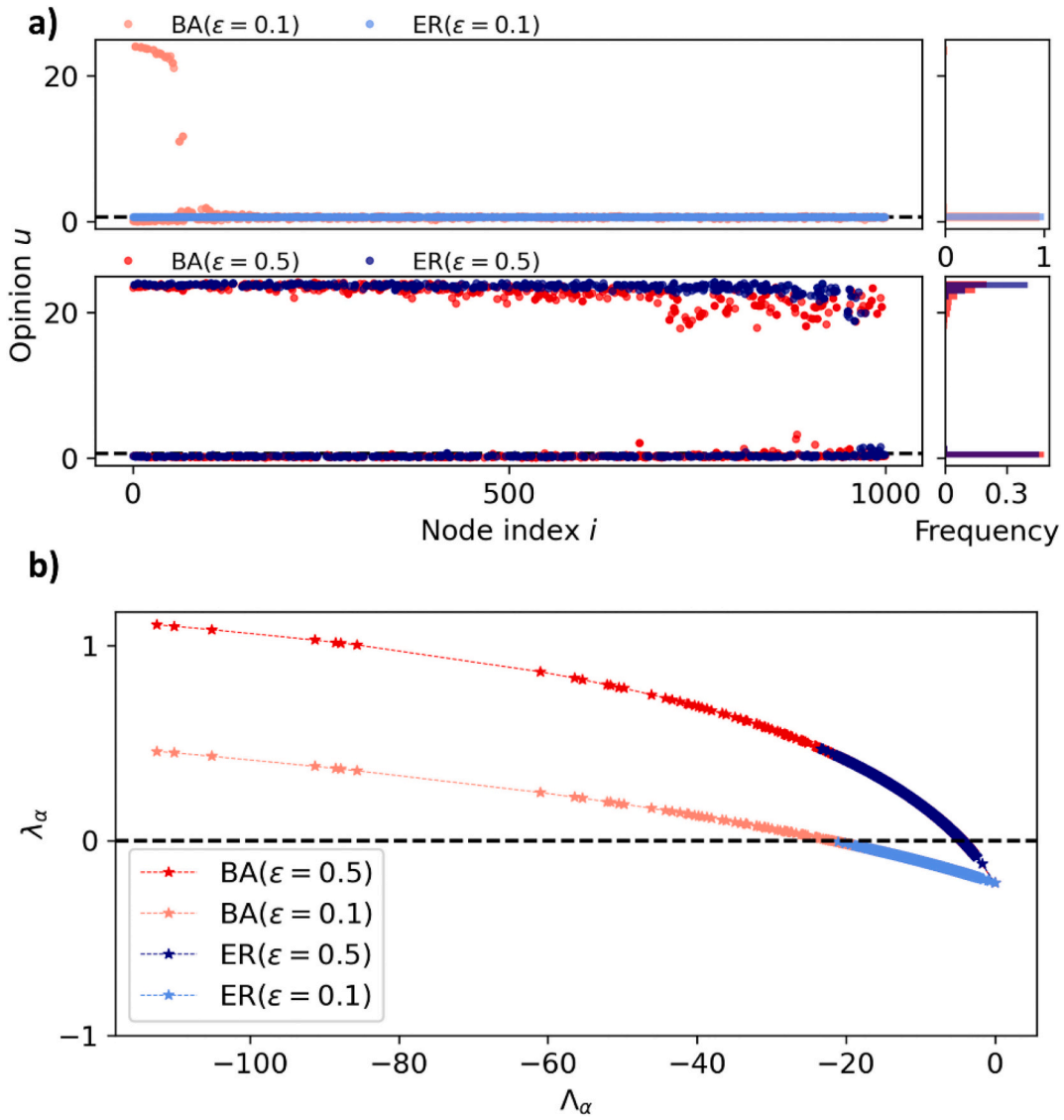

Fig. 1. Turing instability for two different topologies, the Erdos-Renyi (ER) in blue, and the Barabasi-Albert (BA) in red, with size $N = 1000$. In panel (a), two different values of the network influence are considered, $\epsilon = 0.1$ and $\epsilon = 0.5$. Right sub-panels represent the histograms of each distribution. Panel (b) shows the growth rate distribution associated to each configuration of panels in (a). For these simulations, $c = 0.27$, $d_{uv} = 0.0$ and $d_{vu} = 0.17$. Both networks have a mean degree of $k \simeq 10$ and the nodes are shown in a decreasing order of their connectivity value. The black dashed line in panel (a) represents the fixed stable point of the system for the given parameters, $u^0 = 0.62$, while in panel (b) is a visual aid to see when the growth rates become positive. (For interpretation of the references to color in this figure legend, the reader is referred to the web version of this article.)

panels (d-f) show that the region of positive GR indeed outlines the onset of polarization. As we saw in Fig. 1, for $\epsilon = 0.1$ only nodes with large connectivities in the BA network had started to adopt new opinions, but since the overall opinion distribution remains practically unimodal, the polarization index is considerably small, around $\mu = 0.25$. It is interesting to see, however, that in the ER network the colored region with non-zero polarization index is smaller than the BA but higher in value, reaching $\mu = 0.5$. This feature is highlighted in the bottom panels with $\epsilon = 0.5$, where μ can reach the unity in the WS network but not in the BA. Again, this is related to the connectivity distribution and its dispersion, being in some way the opposite case of what we had earlier. Now, the less connected nodes of the BA are the last to adopt one of the extreme opinions and they are still in the fixed point, contributing to the noise of the opinion distribution and decreasing the distance between the opinion clusters. For the ER and WS networks, if the network influence is large enough so the mean connectivity of the network is above a critical value, almost all nodes will adopt one of the extreme opinions leaving as a result a clear bimodal distribution, which in turn result in a higher polarization index. In the case of the WS, since the dispersion in connectivity is even smaller (see *Supplementary Information* Fig. S1), the dispersion in the opinion clusters is also smaller and thus the distance between them is maximal. Besides, the color patterns of panels *k* and *l* reflect mainly on whether the opinion clusters are equally populated or not, with the cross-diffusion parameter d_{vu} acting as a driving force that makes one of the opinion clusters bigger than the other.

Going back to the Turing patterns, Fig. 3 collects several panels in which we study the effect of different model parameters on the size of the Turing area measured at the parameter space in Fig. 2. First, we examine its growth as a function of the network influence ϵ, where we see how in the BA it grows faster and saturates earlier around the value of 0.65, the one previously shown in Fig. 2g. For the ER and WS, we also examine its growth over the network average connectivity (with fixed $\epsilon = 0.1$) and see that the region with positive GR in the WS model is slightly smaller than in the ER and that it also grows slower with the network influence ϵ. As we mentioned earlier, these two parameters interplay with each other in the sense that ϵ modifies the threshold for

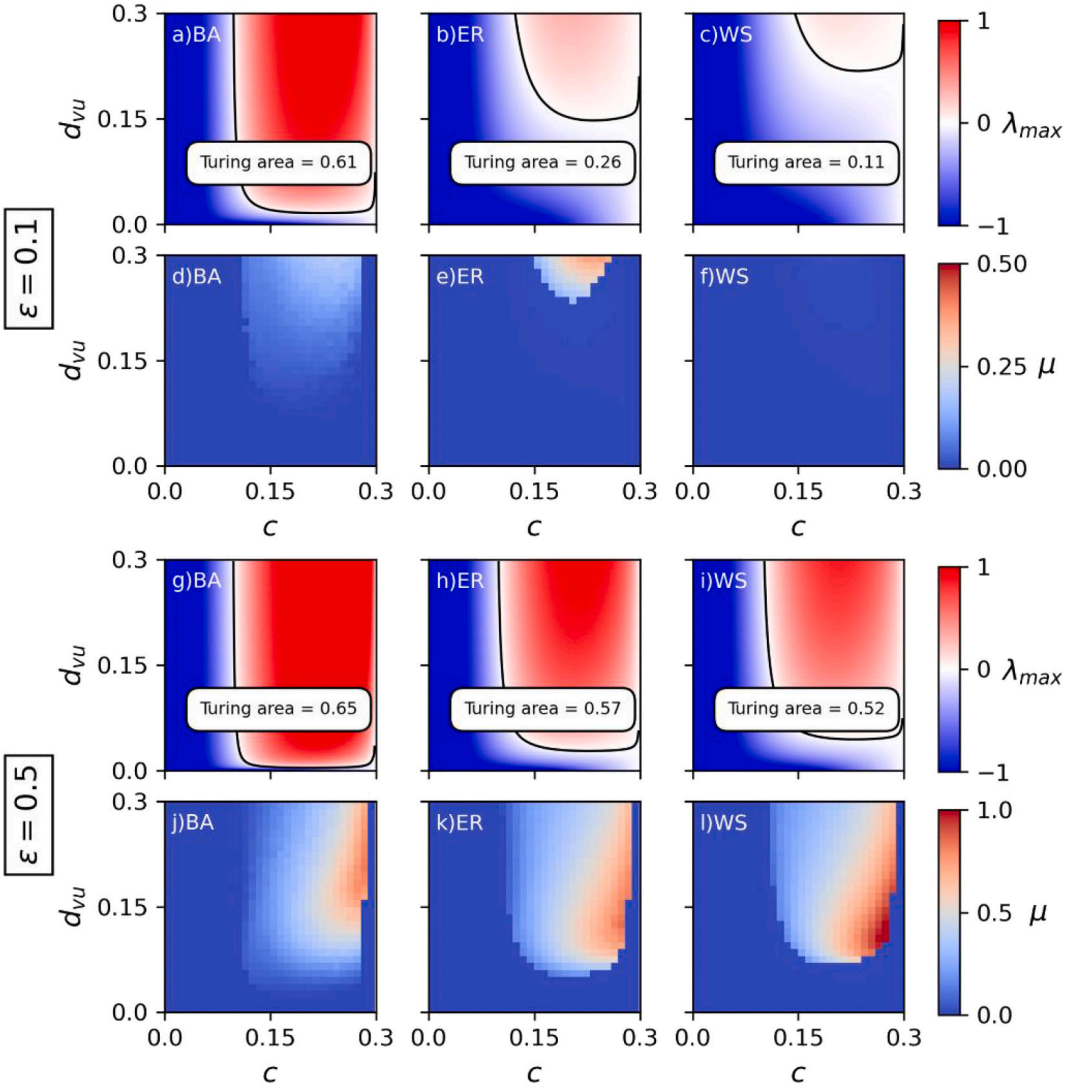

Fig. 2. Maxima of the growth rates λ_{max} (a-c and g-i) and polarization index μ (d-f and j-l) in the parameter space of the model for $\epsilon = 0.1$ and $\epsilon = 0.5$, for three different network topologies. BA accounts for Barabasi-Albert, ER for Erdos-Renyi and WS for Watts-Strogatz. Here, network size was fixed to $N = 5000$ for all panels because of size effects (see panel 3a). Note that in panels (d-f) the colormap was adjusted between $\mu = 0$ and $\mu = 0.5$ to zoom in the values of panels d-e.

the positive growth rates λ_c, and for these two network models an increase in the average connectivity conveys an increase in the maximum growth rate λ_{max}. Thus, increasing any of these two parameters makes it easier for these networks to reach the onset of polarization and enlarge their Turing area. Besides, the difference among them can be closely related to the average pathlength ℓ suggesting that the time scale of the information flow, that is minimized in the BA model due to the presence of hubs, is also one of the key features in the emergence of the Turing instability and, thus, polarized non-homogeneous structures. Using the WS model as a reference, we can increase the average path length of the network by minimizing the number of existing shortcuts. In panel 3d, we compare the size of the Turing region against the average path length for WS networks and show that, in fact, there exists an inverse proportionality between the two of them. This effect has been previously observed in diffusing epidemics [50,51] and it is related to the fact that decreasing the number of shortcuts halts the percolation of the system, which in our case, relates directly with the effective diffusion coefficient and so to the emergence of the Turing patterns. The effect of the network size is also shown in panel 3c, with the outcome that only the BA network experiences a significant change in the Turing region at small sizes. This is again related to the connectivity in the largest hub: the larger the network the bigger their hubs and therefore the more accessible is the onset of polarization. The effect of other model parameters in the Turing area, such as the growth a, simple diffusion or cross diffusion from u to v is left for the *Supplementary Information* Fig. S2. From a certain value, well below the one used in our main results, increasing the growth a has no effect in the size of the Turing area. On the other hand, increasing simple diffusion and cross diffusion d_{uv} tends to stabilize the system and remove heterogeneities, thus inhibiting the Turing instability for all three networks equally. We remind that we are not intending to use the Turing stability as a direct explanation of the polarization process but rather as a tool that could measure it, and so we fixed these parameters at a certain value that allowed us to clearly exemplify our method.

Finally, we pay some attention to show how the directionality of the links affects our model and inspect further the connection between a critical connectivity and polarizing effects. It is usual that users online communicate unilaterally, following someone who do not follow back or answering a post which do not receive another answer in return. We have seen that the degree heterogeneity above a certain critical value is a necessary condition for the polarization to occur, and our model is very susceptible to the directionality of the interactions. Attending to Eq. (1), node i modifies its opinion in function of those nodes that i is looking up to, given by the rows of the adjacency matrix A_{ij} which represent the out-

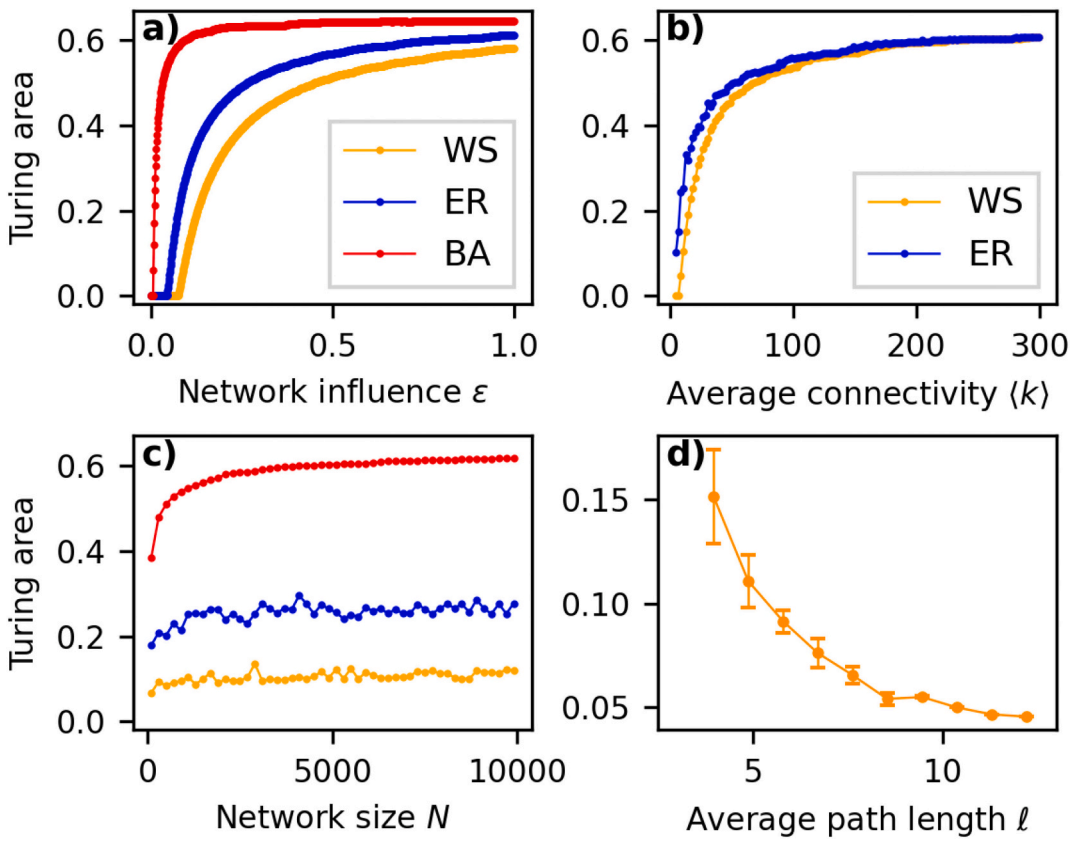

Fig. 3. Size of the Turing area in function of the network influence (a), average network connectivity (b), network size (c) and average path length ℓ (d). For panels a, b and d, network size was fixed at $N = 5000$, while for panels b, c and d network influence was fixed at $\epsilon = 0.1$. Error bars in panel (d) account for multiple realizations of the network with very similar ℓ.

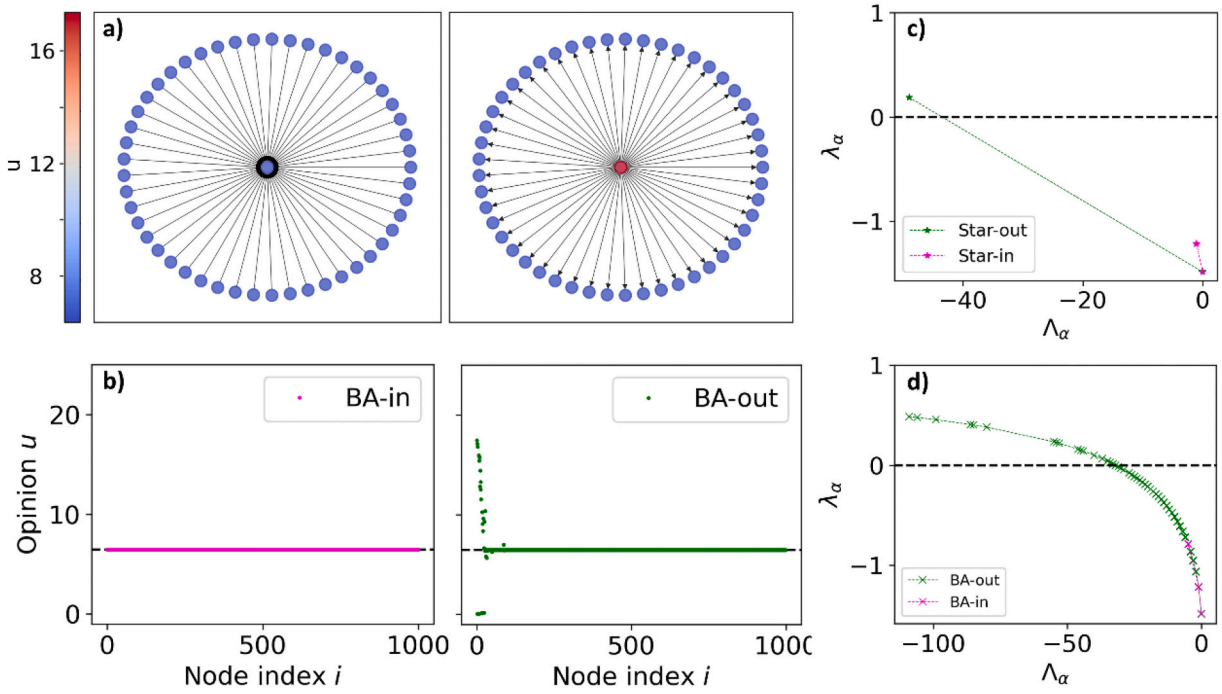

Fig. 4. Effects of the link direction in the model. In star graphs (a) with $k = 50$, inward direction results in consensus while outward direction in polarization of the central node when $k_{central}$ is higher than a critical value. This can be extrapolated to BA directed networks (c), where hubs with outward connectivity larger than a critical one become polarized while the rest of the nodes do not. Panels (b) and (d) show the growth rate distribution for each case. In all panels, $\epsilon = 0.1$, while network size is $N = 50$ for the star networks and $N = 1000$ for the BA networks.

connectivity of i. Therefore, for each node, the opinion diffusion depends only on its outwards connectivity. In turn, the sum of connections that are following the opinion of node i and given by the columns of A_{ij}, account for the in-connectivity of the node and have no relevance in its opinion value since they do not affect the equations. In the case of social networks, this could represent a mechanism by which the opinion of a given user would be purely affected by how much activity they engage into rather than by the attention they receive. Using directed star networks, we can highlight the latter to find that the central node is always potentially polarized (exhibits a differentiated state of opinion) whenever it is the out-connectivity the one higher than the critical threshold (which is found near the critical value of the Laplacian eigenvalue, $k_c \simeq \Lambda_c$), while if the central node only possesses inward connectivity, the polarization does not occur (see Fig. 4 panels (a) and (c)). The result is that the outward star network always has a positive growth factor if $k > k_c$ (green points) while the inward star graph does not (pink points). This outcome extrapolates to directed scale free networks, as panels (c) and (d) show. As in Fig. 1, the nodes in panel (c) are ordered in function of their connectivity, in descending order. Here, hub nodes with high out-connectivity are found polarized while nodes with small-to-none out-degree are found at the fixed point without the slight dispersion previously observed at in Fig. 1a). In the opposite case of a scale-free graph with fixed low out-connectivity and a power law distributed in-connectivity, the consensus remains and the network does not polarize. Notice however that although here the outward's is the preferential direction predefined by the model itself, it could be arranged otherwise so the preferential direction was the inward's and the outcome would be conceptually the same.

4. Conclusions

We defined the size of the parameter space where the Turing instability takes place as a measurement of the potential of polarization of a given network in the sense of exhibiting non-homogeneous opinions. For this, we endowed the nodes with the dynamics of a simple model where two opposing ideas compete for being the prevalent one and the system can end up either in a consensus or in a differentiated state. The second one appears only once the diffusion has been turned on in the system via the Turing instability, and thus through the study of the instability patterns we mapped the parameter space in which the network is sustaining the polarized state. Then, to exemplify our approach, we considered different network models and checked the sensitivity of our descriptor to topological variations in the network structure, showing how intrinsic features such as the node degree or the average path length affected our measurements. From this point of view, besides presenting the method, our computations suggest that the more compact the network is in terms of its average path length, the more accessible is the polarized state. In this way, a network structure with a scale-free connectivity distribution appears to be more prone to polarization because of the presence of hubs, which acts as important shortcuts for information diffusion and reduce drastically the average shortest path. On the other hand, connectivity patterns also hold great importance, and we show that both the average connectivity and its dispersion are key to reach the onset of polarization and sustain clear polarized structures. As we discussed in detail in the previous section, larger node degrees allow for larger Laplacian eigenvalues and more localized eigenvectors, which causes those nodes to differentiate faster. This is highlighted by specifying the link direction, where we show that opinion polarization strictly occurs in the direction where the exchange of opinions occurs and when the outward connectivity of a given node is high enough to overcome a critical threshold. With the help of star-shape and scale-free networks, we show that the nodes with higher interactions pointing outwards become rapidly polarized while the rest remain at their original consensus state. In this sense, we see that it is the intrinsic features of the node which drives them to become polarized, but from this state they don't seem to be able to polarize their low-activity neighbors. In other words, here the Turing instability detects which nodes have polarized in the circumstances given by the network parameters, which will be those that seem to have overcome the critical threshold in connectivity. A suitable physical interpretation of this outcome could have been empirically observed before, where highly active users, more engaged in online discussions, are the ones that tend to present more extreme opinions [30]. In what regards the Erdos-Renyi and Watts-Strogatz network models, we see that although their Turing area is noticeably smaller than in the BA, they reach higher values in the polarization index proposed by [19]. The cause of this is again related to the connectivity distribution and the small dispersion present in these two network models. While Fig. 1 shows that the onset of polarization in the BA occurs following a descending order in connectivity, in these other two networks the instability affects all nodes equally forcing everyone to adopt one of the new states, reducing the noise in the system and increasing the distance between the opinion clusters. As a final note, although our descriptor is limited in discerning how much polarized the state is based on the previous definition, it does offer a suitable and efficient tool to bound the onset of polarization in the parameter space of the model without the need to perform any extensive simulation.

Our method and the Turing instability shows that a particular network topology is no longer fitted to support a consensus state and, thus, should evolve into a non-homogeneous configuration that we associate with polarization. A possible extension of this method could be envisioned to understand and describe the existence of multiple opinions when a more complex dynamical model is considered allowing multiple states.

It is important to note that here the Turing instability is not intended as an explanation of the polarization dynamics (although it may) but as a means to quantify topological differences between different networks that describe different situations in real human relations. We believe that our results may contribute to quantify this important magnitude and help compare levels of polarization in different contexts. Future work with online social networks is intended, hoping that our research may contribute to understanding why the levels of polarization in our societies seem to be steadily increasing.

CRediT authorship contribution statement

A. Carballosa performed most of the simulations, drew the figures and wrote the first draft of the manuscript. A. Crego contributed in the initial steps of the work. APM proposed the original idea. All authors contributed in the discussion of the results and the writing.

Declaration of competing interest

The authors declare that they have no known competing financial interests or personal relationships that could have appeared to influence the work reported in this paper.

Data availability

No data was used for the research described in the article.

Acknowledgements

We gratefully acknowledge financial support by the Spanish Ministerio de Economía y Competitividad and European Regional Development Fund under contract RTI2018-097063-B-I00 AEI/FEDER, UE, and by Xunta de Galicia under Research Grant No. 2021-PG036. All these programs are co-funded by FEDER (UE). A. Carballosa acknowledges financial support from Xunta de Galicia. The simulations were run in the Supercomputer Center of Galicia (CESGA) and we acknowledge their support.

Appendix A. Supplementary data

Supplementary data to this article can be found online at https://doi.org/10.1016/j.chaos.2023.113697.

References

[1] R. Hegselmann and U. Krause, "Opinion dynamics and bounded confidence: models, analysis and simulation," JASSS J. Artif. Soc. Soc. Simul., vol. 5, p. 2, June 2002.
[2] Fiorina MP, Abrams SJ. Political polarization in the American public. Annu Rev Polit Sci June 2008;11:563–88.
[3] Lee FE. How party polarization affects governance. Annu Rev Polit Sci 2015;18:261–82.
[4] Poole K, Rosenthal H. The polarization of American politics. J Polit May 1983;46.
[5] Baldassarri D, Gelman A. Partisans without constraint: political polarization and trends in American public opinion. Am J Sociol September 2008;114:408–46.
[6] McCarty N, Poole KT, Rosenthal H. Polarized America: The Dance of Ideology and Unequal Riches. Cambridge, MA: MIT Press; 2006.
[7] DiMaggio P, Evans J, Bryson B. Have American's social attitudes become more polarized? Am J Sociol November 1996;102:690–755.
[8] Abramowitz AI, Saunders KL. Is polarization a myth? J Polit April 2008;70:542–55.
[9] Lelkes Y. Mass polarization: manifestations and measurements. Public Opin Q January 2016;80:392–410.
[10] Prior M. Media and political polarization. Annu Rev Polit Sci May 2013;16:101–27.
[11] Sunstein CR. #republic: Divided democracy in the age of social media. Princeton University Press; 2018.
[12] T. Sonnemaker, 11 experts explain how our digital world is fueling polarization.
[13] de-Wit L, Cameron Brick S van der Linden a. Are social media driving political polarization?. 2019.
[14] Boxell L, Gentzkow M, Shapiro JM. Greater internet use is not associated with faster growth in political polarization among US demographic groups. Proc Natl Acad Sci October 2017;114:10612–7.
[15] Weng L, Flammini A, Vespignani A, Menczer F. Competition among memes in a world with limited attention. Sci Rep March 2012;2:335.
[16] Lorenz-Spreen P, Mønsted BM, Hövel P, Lehmann S. Accelerating dynamics of collective attention. Nat Commun April 2019;10:1759.
[17] Conover M, Ratkiewicz J, Francisco M, Goncalves B, Menczer F, Flammini A. Political polarization on Twitter. In: Proceedings of the International AAAI Conference on Web and Social Media. 5; 2011. p. 89–96.
[18] Guerra PH, Meira Jr W, Cardie C, Kleinberg R. A measure of polarization on social media NetworksBased on community boundaries. In: Proceedings of the 7th international conference on weblogs and social media, ICWSM 2013; January 2013. p. 215–24.
[19] Morales AJ, Borondo J, Losada JC, Benito RM. Measuring political polarization: twitter shows the two sides of Venezuela. Chaos March 2015;25:033114.
[20] Degroot MH. Reaching a consensus. J Am Stat Assoc March 1974;69:118–21.
[21] Friedkin N, Johnsen E. Social influence and opinions. J Math Sociol January 1990;15:193–206.
[22] McPherson M, Smith-Lovin L, Cook JM. Birds of a feather: homophily in social networks. Annu Rev Sociol August 2001;27:415–44.
[23] Axelrod R. The dissemination of culture: a model with local convergence and global polarization. J Confl Resolut April 1997;41:203–26.
[24] Bessi A, Petroni F, Vicario MD, Zollo F, Anagnostopoulos A, Scala A, et al. Homophily and polarization in the age of misinformation. Eur Phys J Special Topics October 2016;225:2047–59.
[25] Dandekar P, Goel A, Lee DT. Biased assimilation, homophily, and the dynamics of polarization. Proc Natl Acad Sci April 2013;110:5791–6.
[26] Vicario MD, Bessi A, Zollo F, Petroni F, Scala A, Caldarelli G, et al. The spreading of misinformation online. Proc Natl Acad Sci January 2016;113:554–9.
[27] Cota W, Ferreira SC, Pastor-Satorras R, Starnini M. Quantifying echo chamber effects in information spreading over political communication networks. EPJ Data Sci December 2019;8:1–13.
[28] Cinelli M, Morales GDF, Galeazzi A, Quattrociocchi W, Starnini M. The echo chamber effect on social media. Proc Natl Acad Sci March 2021;118.
[29] Del Vicario M, Vivaldo G, Bessi A, Zollo F, Scala A, Caldarelli G, et al. Echo chambers: emotional contagion and group polarization on Facebook. Sci Rep December 2016;6:37825.
[30] Baumann F, Lorenz-Spreen P, Sokolov IM, Starnini M. Modeling Echo chambers and polarization dynamics in social networks. Phys Rev Lett January 2020;124:048301.
[31] Lord CG, Ross L, Lepper MR. Biased assimilation and attitude polarization: the effects of prior theories on subsequently considered evidence. J Pers Soc Psychol 1979;37:2098–109.
[32] Musco C, Musco C, Tsourakakis CE. Minimizing polarization and disagreement in social networks. In: Proceedings of the 2018 world wide web conference. Republic and Canton of Geneva, CHE; 2018.
[33] Santos FP, Lelkes Y, Levin SA. Link recommendation algorithms and dynamics of polarization in online social networks. Proc Natl Acad Sci December 2021;118.
[34] McCright AM, Dunlap RE. The politicization of climate change and polarization in the American public's views of global warming, 2001–2010. Sociol Q May 2011;52:155–94.
[35] Garimella K, Morales GDF, Gionis A, Mathioudakis M. Quantifying controversy on social media. In: ACM transactions on social computing. vol. 1; January 2018. 3:1–3:27.
[36] Turing A. The chemical basis of morphogenesis. Philoso Trans R Soc Lond B Biol Sci August 1952;237:37–72.
[37] Murray J. Mathematical biology. Berlin-Heidelberg: Springer-Verlag; 1993.
[38] Vidal-Franco I, Guiu-Souto J, Muñuzuri AP. Social media enhances languages differentiation: a mathematical description. R Soc Open Sci May 2017;4:170094.
[39] Sayama H, Pestov I, Schmidt J, Bush BJ, Wong C, Yamanoi J, et al. Modeling complex systems with adaptive networks. Comput Math Appl May 2013;65:1645–64.
[40] Mimar S, Juane MM, Park J, Muñuzuri AP, Ghoshal G. Turing patterns mediated by network topology in homogeneous active systems. Phys Rev E June 2019;99:062303.
[41] Vanag VK, Epstein IR. Cross-diffusion and pattern formation in reaction–diffusion systems. Phys Chem Chem Phys January 2009;11:897–912.
[42] Wang W, Lin Y, Zhang L, Rao F, Tan Y. Complex patterns in a predator–prey model with self and cross-diffusion. Commun Nonlinear Sci Numer Simul April 2011;16:2006–15.
[43] Xue L. Pattern formation in a predator–prey model with spatial effect. Phys A Stat Mech Appl December 2012;391:5987–96.
[44] Ruiz Baier R, Tian C. Mathematical analysis and numerical simulation of pattern formation under cross-diffusion. Nonlinear Anal Real World Appl February 2013;14.
[45] Nakao H, Mikhailov AS. Turing patterns in network-organized activator–inhibitor systems. Nat Phys July 2010;6:544–50.
[46] Erdös P, Rényi A. On random graphs I. Publ Math Debr 1959;6:290–7.
[47] Barabási A-L, Albert R. Emergence of scaling in random networks. Science October 1999;286:509–12.
[48] Barabási A-L, Pósfai M. Network Science. Cambridge University Press; 2016. p. 112–63.
[49] Watts DJ, Strogatz SH. Collective dynamics of 'small-world' networks. Nature June 1998;393:440–2.
[50] Moore C, Newman ME. Epidemics and percolation in small-world networks. Phys Rev E Stat Phys Plasmas Fluids Relat Interdiscip Top May 2000;61:5678–82.
[51] Carballosa A, Mussa-Juane M, Muñuzuri AP. Incorporating social opinion in the evolution of an epidemic spread. Sci Rep January 2021;11:1772.